Interference Analysis of EHF/THF Communications Systems with Blocking and Directional Antennas

V. Petrov*, M. Komarov*, D. Moltchanov*, J. M. Jornet†, Y. Koucheryavy*
*Tampere University of Technology, Tampere, Finland,
Email: {vitaly.petrov, dmitri.moltchanov}@tut.fi, yk@cs.tut.fi
†University of Buffalo, USA, Email: jmjornet@buffalo.edu

***Abstract*—The fifth generation wireless systems are expected to rely on a large number of wideband small cells to offload traffic from the cellular and wireless local area networks. To create such small cells, EHF and THF bands are actively explored. These frequencies are characterized by fundamentally different propagation characteristics resulting in different interference structure at the receiver compared to, e.g., microwave systems. In this paper, we study the interference structure for systems operating in EHF/THF bands by explicitly capturing three major phenomena: (i) extreme directivity of the transmit and/or receive antennas, (ii) pass loss component caused by molecular absorption and (iii) blocking of high-frequency radiation. The metric of interest is the mean interference at the receiver. Our results reveal that (i) for the same emitted energy in a Poisson field of interferers, the interference increases with the directivity of the transmit or receive antennas, (ii) blocking has a profound impact on the interference creating much more favorable conditions for communications compared to lower frequencies and (iii) the choice of the antenna model is of crucial importance for accurate performance assessment.**

I. Introduction

To keep up with constantly increasing traffic demands and quality of service requirements [1], industry is preparing for a 1000x increase in mobile data [2]. In spite of a significant step forward, even the current 4G cellular technologies will soon be insufficient to satisfy the constantly growing devices base and customer traffic demands. The future generation of wireless systems is expected to rely on small cells to offload heavy traffic from the cellular and even local area networks. To enable this, the so-called millimeter wave systems operating in the lower part of EHF band, $30-300$GHz, are currently under standardization. Several wireless communication actors are already investigating the use of even higher frequencies available in the terahertz band (THF, $0.3-3$THz), e.g., 300GHz, 640GHz, and even the entire THz band [3], [4], [5].

The THz band is characterized by several unique features [6] and there are a number of critical factors affecting waves propagation in EHF and THF bands. First, the line-of-sight (LoS) signal in these bands can be effectively blocked by almost any obstacle, including walls, furniture and human bodies. Effectively, any object whose size is greater than few millimeters acts as a blocker. The recent measurement and ray-tracing simulation campaigns report that up to $60 \sim 80\%$ of energy available at the receiver comes from the LoS component [7], [8]. While reflections off the objects in the channel do contribute, their effect is of secondary importance and presence of LoS often dictates the channel quality [7].

The second inherent feature of the considered bands is molecular absorption. The phenomenon is related to absorption of electromagnetic energy by the molecules in the environment having resonant frequencies in the communications band of interest. In EHF band, oxygen, that is abundant in the atmosphere, affects the path loss. The net result is additional $10-20$dB loss per kilometer [7]. For THF band the molecules of water vapor serves the role of primary absorbent [9]. Irrespective of the the type of absorbent the resulting effect is more complex expression for the power at a the receiver.

Finally, transmitters operating in EHF/THF bands are characterized by high antenna directivity allowing to partially overcome severe propagation losses. At the same time, when the beam is extremely narrow, there is the need for complex electronic beamsteering to maintain the channel between the transmitter the receiver. The narrower the beam the more precise system is needed and, at the same time, the less interference for other stations the current transmission incurs. To understand the trade-off between the directivity angle of antennas, the requirements imposed on beamsteering system and the interference models for directional antennas are needed.

To the best of the authors' knowledge there are no studies simultaneously capturing the effect of the abovementioned phenomena on interference experienced at the receiver. In this paper, using the tools of stochastic geometry, we address the question of interference analysis for systems operating in EHF and THF bands explicitly capturing the following three effects inherent for these frequencies: (i) directivity of the transmit and receive antennas, (ii) path-loss component caused by molecular absorption and (iii) blocking of high frequency radiation. Two models of directional transmit antennas capturing the propagation effects with different details are addressed. The metric of interest is mean interference at the receiver obtained in closed-form as a function of the antenna model, antenna directivity, density of interferers in the environment.

The rest of the paper is organized as follows. In Sec. II we recall the propagation characteristics of EHF and THF bands, introduce antenna and network models. The interference is analyzed in Sec. III. Numerical results are reported in Sec. IV. The conclusions are drawn in the last section.

978-1-5090-1328-9/16/$31.00 ©2016 IEEE

TABLE I
NOTATION USED IN THE PAPER.

Parameter	Definition
System parameters	
P_{Tx_0}	Emitted power at the tagged transmitter
P_{Rx_0}	Received power at the tagged receiver
r_0	The distance between Rx_0 and Tx_0
r_i	The distances between interferers/blockers and Rx_0
r_B	Radius of interferer/blocker
$r^\star$	Radius for side lobe approximation
R	The interference zone around the tagged receiver
λ	The density of interferers/blockers in the area
Propagation model parameters	
K	Absorption coefficient, $K \in (0, 1)$
$S_{Rx}(f, r)$	Received psd
$L_P(f, r)$	Free-space propagation losses
$L_A(f, r)$	Absorption losses
$\tau(f, r)$	Transmittance of the medium
f	Operational frequency
Antenna model parameters	
A, A_1, A_2	Antenna coefficients
k	Coefficient of losses to the side lobes, $k \in (0, 1)$
α	Antenna directivity angle
Blocking model parameters	
l_A	Length of an arc of the circumference
λ_P	Intensity of projections of blockers
L	Distance from the receiver to a blocker
W	Blocked interval created by a single blocker
B, A	Length of blocked and non blocked intervals
v_i	Renewal points associated with blocking process
$p_B(x), p_A(x)$	Probability that a random point in blocked/not blocked
Interference model parameters	
I	Aggregate interference
p_C	Probability that interferer affects Rx_0
Λ	Intensity of the unblocked interferers
$r_\star$	Radius of side lobe's effect
N	Number of interferers in the circle of radius R
N_O	The overall number of interferers affecting Rx_0

II. Propagation, Antenna and Network Models

The notation used in the paper is summarized in Table I.

A. Propagation in EHF/THF Bands

The distinguishing feature of the EHF/THF channels is presence of the molecular absorption loss [10], [11], albeit much stronger in THF band. In THF band these losses are mainly caused by H_2O vapor in the air while in EHF band, especially, in unlicensed 60GHz band, it is dominated by O_2 molecules. These losses make wireless channels extremely frequency selective. The received power spectral density (psd) in the EHF/THF band can written as

$$S_{Rx}(f, r) = \frac{S_{Tx}(f)}{L_A(f, r)L_P(f, r)}, \tag{1}$$

where f is the operating frequency, r is the separation distance between the transmitter and the receiver, $S_{Tx}(f)$ stands for the transmitted signal psd, $L_A(f, r)$ represents the absorption loss, and $L_P(f, r)$ is the propagation loss that depends on the antenna directivity.

Following [10], the absorption loss is defined as

$$L_A(f, r) = \frac{1}{\tau(f, r)}, \tag{2}$$

where $\tau(f, r)$ is the transmittance of the medium following the Beer-Lambert law, $\tau(f, r) \approx e^{-K(f)r}$, where $K(f)$ is the overall absorption coefficient of the medium available, for instance, from HITRAN database [12].

B. Antenna models

In our study we consider the following antenna models:

- cone model;
- cone-plus-sphere.

In the first model, the directivity of the transmitter is taken into account considering the coverage zone to be of cone-shape as shown in Fig. 1(a). This model is an abstraction assuming no side lobes and constant power at a certain separation distance from the transmitter. The second model, illustrated in Fig. 1(b), takes into account imperfect antenna radiation pattern by modeling side lobes as a sphere around the antenna. Still, the power of the main lobe is assumed to be constant and depend on the distance from the antenna only.

To parameterize the cone antenna model, we need to provide coefficient A corresponding to a directivity angle α of the antenna. For the second model, A_1 and A_2, corresponding to the main and side lobes, respectively, have to be provided. Coefficients A, A_1, and A_2 will be later used in the propagation model to properly amplify the signal with respect to the direction it goes to or comes from.

1) Cone Antenna Model: For this antenna type, the surface area of a wavefront can be expressed as

$$S_A = \frac{P_{Tx}}{P_{Rx}} = 2\pi r h, \tag{3}$$

where P_{Tx} refers to the total transmitted power, P_{Rx} refers to the power density at the wavefront, $h = r[1 - \cos(\alpha/2)]$ and α is the antenna directivity angle.

According to free-space propagation loss model (FSPL), the power density at the wavefront is given by

$$P_{Rx} = \frac{P_{Tx}}{S_A} = \frac{A}{4\pi} r^{-2} P_{Tx}, \tag{4}$$

which implies that the parameter A is given by

$$A = \frac{2}{1 - \cos(\alpha/2)}. \tag{5}$$

2) Cone-Plus-Sphere Antenna Model: To parameterize this antenna model we need to find A_1 and A_2. Denoting the fraction of energy concentrated along the main lobe by k_1 and the one lost to side lobes by k_2, we formulate the following set of equations:

$$\begin{cases} P_{Rx1} 2\pi r^2 [1 - \cos(\alpha/2)] = k_1 P_{Tx} \\ P_{Rx2} 2\pi r^2 [1 + \cos(\alpha/2)] = k_2 P_{Tx} \\ k1 + k2 = 1 \end{cases}, \tag{6}$$

where, according to the FSPL,

$$\begin{cases} P_{Rx1} = A_1 r^{-2} P_{Tx}/4\pi \\ P_{Rx2} = A_2 r^{-2} P_{Tx}/4\pi \end{cases}. \tag{7}$$

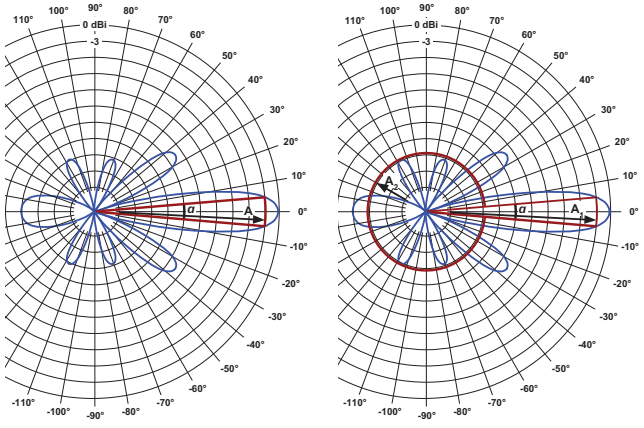

(a) Cone (b) Cone-Plus-Sphere (CPS)

Fig. 1. Illustration of the considered antenna models.

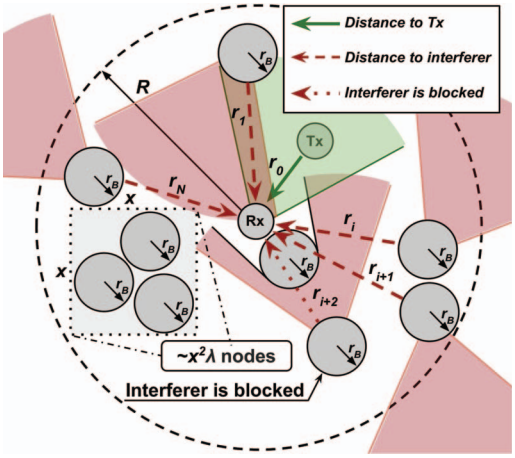

Fig. 2. An illustration of the considered network deployment.

Thus, we have the following relation between A_1 and A_2

$$A_1[1-\cos(\alpha/2)] + A_2[1+\cos(\alpha/2)] = 2. \quad (8)$$

There are multiple solutions for (A_1, A_2). Setting $A_2 = 0$ reduces the model to cone antenna. Introducing $k = k_1/k_2$, $k \in (0,1)$ we see that $A_2 = kA_1$ and A_1, A_2 are

$$\begin{cases} A_1 = 2[(1-\cos(\alpha/2)) + k(1+\cos(\alpha/2))]^{-1} \\ A_2 = kA_1 \end{cases}. \quad (9)$$

We now have the relations to specify A, A_1, and A_2 as functions of α and k in such a way that total transmit power does not change with the antenna directivity. This allows us to further compare the interference levels in fair conditions.

C. Network Model

As the major emphasis of this study is to assess of the EHF/THF band's communications specifics, we consider a standard random nodes deployment in $\Re^2$, see Fig. 2. We model the field of interferers by a Poisson point process with intensity λ. We tag an arbitrary one and assign it as a receiver of interest, Rx_0. The associated transmitter, denoted as Tx_0, is chosen to be at the distance r_0 from the Rx_0. The rest of the nodes are considered as interferers. To model the respective receivers we assume that the orientation of the bisects of all coverage zones of transmitters are uniformly distributed in $(0, 2\pi)$. The radius of the zone, where the nodes provide non-negligible interferences, R, can be computed using the propagation model. The transmissions of the nodes that are further than R is considered as noise. In our study, we consider interferers acting as blockers to themselves as well, i.e., a certain interferer residing along the path between another interferer and Rx_0 blocks the LoS path. In what follows, depending on the context, the terms blocker and interferer are used interchangeably. The blockers are assumed to be of circular shape with radius r_B, see Fig. 2. The considered scenario corresponds to the case on uncontrolled direct communications in random deployment providing the upper bound on the interference experienced by nodes.

For the described scenario we are interested in the mean value of interference observed at the receiver defined as

$$E[I] = E\left[\sum_{i=1}^{N} A d_i^{-2} e^{-Kd_i}\right]. \quad (10)$$

where N has Poisson distribution with mean $\lambda\pi R^2$.

III. Interference Analysis

A. Blocking Model

Consider the projection of blockers' along the radial lines as shown in Fig. 3. It forms a homogeneous Poisson process even though the intensity of blockers is variable. Indeed, it is easy to prove that the process (i) has marginal Poisson distribution, (ii) is independent at all arc intervals, and (iii) is homogeneous. To demonstrate (i), we observe that the number of points projected at any arc of a fixed length equals to the number of points in the corresponding sector of a circle. The intensity of the blocker's projection on the circumference of the circle of radius x is given by

$$\lambda_P(x) = [S(x) - S(r_B, x)]\frac{1}{l_A}\lambda = \frac{\lambda(x^2 - r_B^2)}{2x}, \quad (11)$$

where $S(x) = l_A x/2$ is the area of the sector with radius x, $S(r_B, x) = l_A r_B^2/2x$ is the area of the difference between sectors of radius x and r_B, l_A is the length of the arc, r_B is the radius of the blocker.

Consider the random variable (RV) W denoting the length of a "shadow'" created by an individual blocker at circumference, in Fig. 4. Observe that it depends on the distance from Tx to the blocker. For $r \gg 2r_B$, where r is the distance from the base of Tx to Rx, we could replace the arc ARxB by a chord AB. Since the points of the Poisson process are uniformly distributed in a circle, the probability density function (pdf) of the distance to a randomly selected blocker is

$$f_L(r; x) = \frac{2r}{x^2 - r_B^2}, \; r_B < r < R. \quad (12)$$

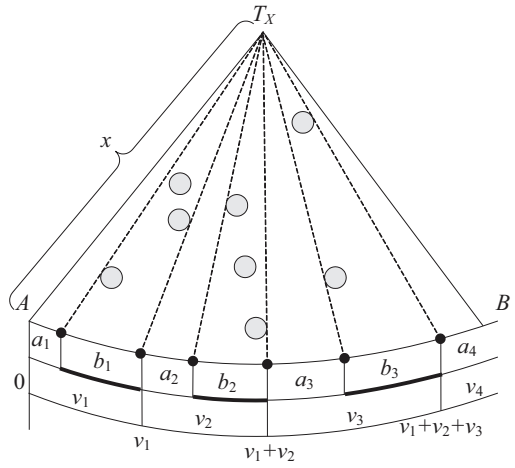

Fig. 3. The renewal process associated with shaded areas.

Observing Fig. 4, by simple geometry we see that

$$W = \frac{2xr_B}{L}, \tag{13}$$

where the distance to the blocker, L, is the only RV involved.

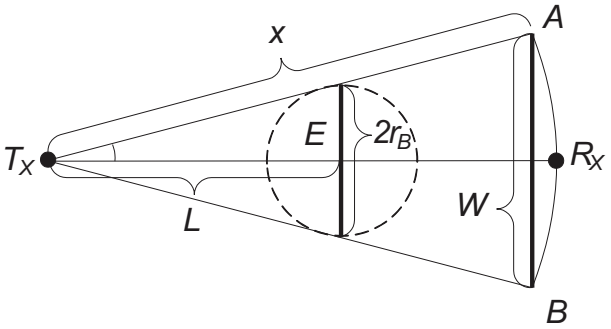

Fig. 4. The length of a blocked part at the circumference.

The density of W can be obtained using the RV transformation technique [13]. Although the inverse function $\psi(y) = 1/x$ has a discontinuity as $x \to 0$ over the domain of L, it is continuous. The modulo of the derivative of $\psi(y)$ is $1/y^2$. Applying non-linear transformation in the form $2r_Bx/L$ the pdf of W can be written as

$$f_W(y;x) = f(\psi(y))|\phi'(y)| = \frac{8x^2r_B^2}{(x^2 - r_B^2)y^3}, \tag{14}$$

and its mean is $E[W(x)] = 4r_Bx/(x + r_B)$. To avoid confusion, from now on, we drop the dependence on the x.

Consider now projections of blockers onto the circumference of radius x, as shown in Fig. 3. The superposed process of all projections forms a renewal process with interchanging blocked and unblocked parts. An arbitrary point on the line is considered blocked if it belongs to one of the blocked interval. We find the probability of blocking at the radius x as the ratio of the means of blocked interval to the sum of the means of blocked and unblocked intervals.

Let a_i b_i, $i = 1, 2, ,$ denote the length of unblocked and blocked intervals respectively, and define $v_i = a_i + b_i$. Points $0, v_1, v_1 + v_2, \ldots, \sum_{j=1}^{N} v_j, \ldots$, are the renewal moments that form the renewal process. The density of this process is [14]

$$f(x) = \lambda_P F_W(x) \exp\left(-\lambda_P \int_0^l [1 - F_W(y)]dy\right). \tag{15}$$

Let $f_V(t)$ be the pdfs of v_i, $i = 1, 2, \ldots$. The functions $f_V(x)$ and $f(x)$ are related to each other via the renewal equation as [14]

$$f(x) = f_V(x) + \int_0^l f_V(x - y)f(y)dy. \tag{16}$$

The length of the unblocked part a_j follows an exponential distribution with parameter λ_P, $F_A(x) = 1 - e^{-\lambda_P x}$. Let $F_B(x)$ and $F_V(x)$ be the CDFs of the length of blocked intervals b_i, and joint blocked/unblocked intervals, V_i, respectively, with means $E[B]$ and $E[V]$. Let further $F_B^*(s)$ and $F_V^*(s)$ be the corresponding Laplace-Stieltjes (LT) transforms. For the joint interval V_i we have

$$F_V^*(s) = F_B^*(s)F_A^*(s) = \lambda_P \frac{F_B^*(s)}{\lambda_P + s}, \tag{17}$$

which can be solved for $F_B(x)$ in the RV domain as

$$F_B(x) = F_V(x) + \frac{f_V(x)}{\lambda_P}. \tag{18}$$

When $l \to \infty$ the renewal density approaches $1/E[V]$. From (15), it also equals to $f(x) = \lambda_P \exp(-\lambda_P E[W])$. Thus,

$$E[V] = \frac{1}{\lambda_P} \exp(\lambda_P E[W]). \tag{19}$$

Consequently, $E[B]$ can now be found as

$$E[B] = \int_0^\infty \left(1 - F_V(x) - \frac{f_V(x)}{\lambda_P}\right) dx = \\ = E[V] - \frac{1}{\mu} = \frac{1}{\lambda_P}[\exp(\lambda_P E[W]) - 1]. \tag{20}$$

The probability of blocking is thus

$$p_B(x) = \frac{E[B]}{E[A] + E[B]} = 1 - e^{-2\lambda r_B(x - r_B)}, \tag{21}$$

where we substituted the mean of W from (14).

The probability of blocking as a function of the distance is shown in Fig. 5. The probability tends to one, when $x \to \infty$. This happens exponentially fast and depends on x and λ.

B. Mean Interference for Cone Antenna Model

Consider the case of directional antenna at either Tx or Rx first. There are two events when an interferer located at distance x does not contribute to the interference at the Rx: (i) its contribution is blocked by other interferers located closely to Rx and (ii) the Rx is not in coverage of the interferer. The former happens with probability p_B. The latter is

$$p_C = \frac{\alpha x}{2\pi x} = \frac{\alpha}{2\pi}, \tag{22}$$

and it is independent of the separation distance x.

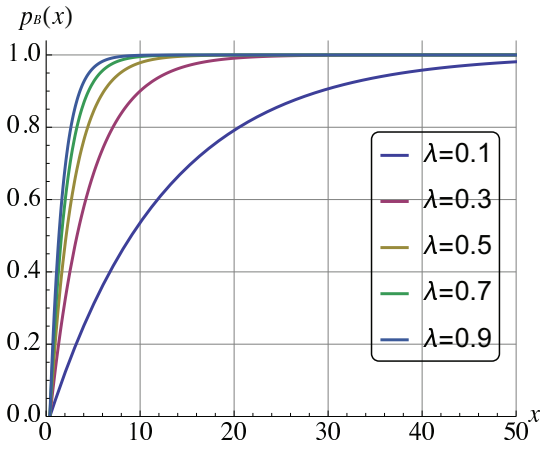

Fig. 5. The probability of blocking as a function of distance.

Consider the infinitesimal radial increment dr. Since the process of blockers/interferers is Poisson multiple events are not allowed to happen within dr and the probability of the event at distance r is proportional to the increment of the area dr. The area increment is given by

$$\pi(r+dr)^2 - \pi r^2 = 2\pi r dr + O(1), \tag{23}$$

implying that the probability of event in $(r, r+dr)$ is $2\lambda\pi r dr$.

When the interferer located at the distance x is not blocked and the Rx is in its coverage area, this contributes $Ar^{-2}e^{-Kr}$ to the interference at the Rx. The mean interference for cone antenna is thus

$$E[I] = \int_{r_B}^{R} Ar^{-2}e^{-Kr}p_C[1-p_B(r)]2\lambda\pi r dr. \tag{24}$$

Substituting (21) and (22) into (24) we get

$$E[I] = \int_{r_B}^{R} Ar^{-2}e^{-Kr}e^{-2\lambda r_B(x-r_B)}\frac{\alpha}{2\pi}2\lambda\pi r dr = \\ = A\alpha\lambda\Theta(R, r_B, \lambda, K), \tag{25}$$

where $\Theta(R, r_B, \lambda, K)$ is given by

$$\Theta = \frac{E(r_B[K+2\lambda r_B]) - E(R[K+2\lambda r_B])}{e^{2\lambda r_B^2}}, \tag{26}$$

and $E(\cdot)$ is the exponential integral.

When blocking is not taken into account, we get

$$E[I] = A\alpha\lambda\int_{r_B}^{R}\frac{1}{r}e^{-Kr}dr = A\alpha\lambda\Theta_1(R, r_B, K), \tag{27}$$

where $Q_1(R, r_B, K) = E(-KR) - E(-Kr_B)$.

When antenna is omnidirectional, we arrive at

$$E[I] = 2\pi\lambda A\Theta(R, r_B, \lambda, K). \tag{28}$$

For omnidirectional antenna and no blocking we have

$$E[I] = 2\pi\lambda A\Theta_1(R, r_B, K). \tag{29}$$

The effect of directional antennas at both Tx and Rx is taken into account by multiplying the expressions, when relevant, by $\alpha/2\pi$. Different directivity at Rx and Tx can be modeled.

C. Cone-Plus-Sphere Antenna Model

For cone-plus-sphere antenna there is a circle around the receiver of radius $r_\star$, where the interferers do not contribute to the overall interference if and only if their contribution is blocked. Thus, for those interferers that are further than $r_\star$ the overall interference is obtained using (25) with the lower limit of integration set to $r_\star$. We denote this component as $E[I_{r_\star<r<R}]$ and its value by $A_1\alpha\lambda\Theta(R, r_\star, \lambda)$. For the component of the interference coming from nodes located within $r_B < r < r_\star$ we have

$$E[I_{r_B<r<r^\star}] = \int_{r_B}^{r_\star} A_1 r^{-2}e^{-Kr}p_C p_A 2\lambda\pi r dr + \\ + \int_{r_B}^{r_\star} A_2 r^{-2}e^{-Kr}(1-p_C)p_A 2\lambda\pi r dr. \tag{30}$$

where A_1 and A_2 are the attenuation coefficients corresponding to main and side lobes. The first integral in (30) has been evaluated in (25) and is given by $A_1\alpha\lambda\Theta(r_\star, r_B, \lambda, K)$. The second is integral, denoted as I_2, given by

$$I_2 = 2A_2\lambda\pi\Theta(r_\star, r_B, \lambda, K) - A_2\alpha\lambda\Theta(R, r_B, \lambda, K) \tag{31}$$

Now, the mean interference for cone-and-sphere antenna is

$$E[I] = [A_1\alpha + A_2(2\pi-\alpha)]\lambda\Theta(R, r_B, \lambda, K). \tag{32}$$

The effect of directional antennas at both Tx and Rx is taken into account by introducing an extra directivity component in (25–32).

IV. Numerical Results

The common belief is that going up in the spectrum and inevitably using directional antennas the operational regime of wireless system will change from interference-limited to noise-limited [15]. In this section, we assess the effects of antenna model, its directivity, and blocking on the mean interference. For comparison purposes throughout this section we present the results assuming that the coefficient A for omnidirectional antenna is set to 1. The results for other antenna models are relative to the omnidirectional one.

A. The Effect of Directivity

The first two figures in Fig. 6 compare the mean interference for scenarios with omni- and directional antennas. The *same emitted power* at all the nodes was assumed, the absorption coefficient was set to $K = 0.01$ and blocking phenomenon was not taken into account. Observing Fig. 6(a) we note that using directional antenna at Tx (or Rx) only results in much larger interference compared to omnidirectional case. Furthermore, the less the directivity angle α the more interference is observed. The reason is that highly directional antennas concentrate the emitted power in a single beam and although only few may affect the receiver, their effect on average is higher compared to omnidirectional antennas. Enabling directivity at both Tx and Rx increases the interference even further and it becomes much higher compared to omnidirectional case. The effect of the density of the nodes is linear for the considered

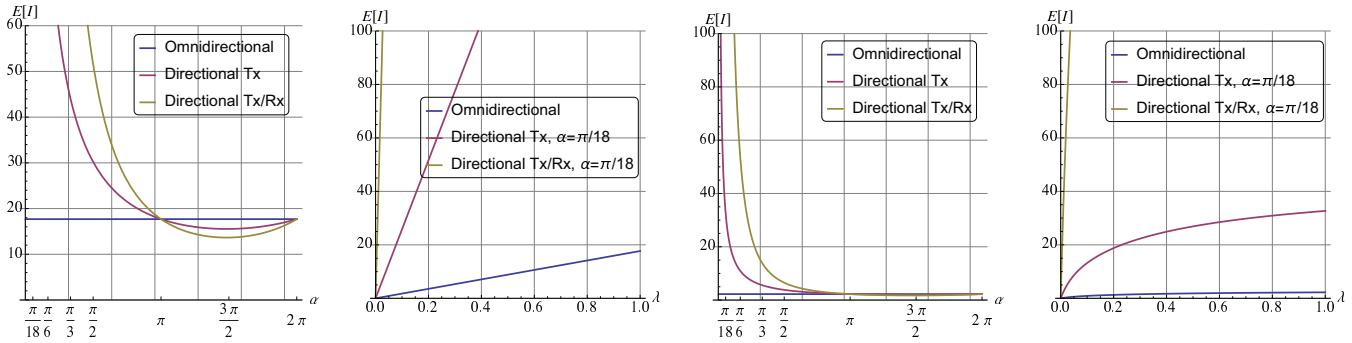

(a) No blocking, varying α, $\lambda = 1$ (b) No blocking, varying λ (c) Blocking, varying α, $\lambda = 1$ (d) Blocking, varying λ

Fig. 6. Comparison of interference for scenarios with omnidirectional and directional (cone) models.

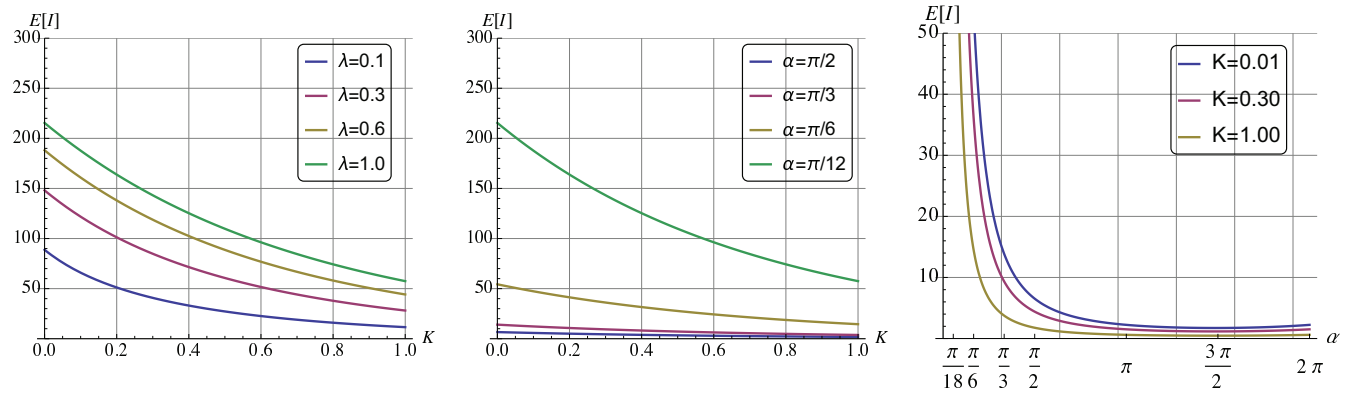

(a) Varying K, $\alpha = \pi/12$ (b) Varying K, $\lambda = 1$ (c) Varying α, $\lambda = 1$

Fig. 7. Dependence of the mean interference on the absorption coefficient K for cone directional antenna model.

cases. The larger the value of λ, the larger the gap between systems with directional and omnidirectional antennas.

This destructive effect of interference is mitigated by: (i) higher received signal strength compared to omnidirectional antennas, (ii) reduction in transmission power and (iii) blocking of EHF/THF radiation by the interferers themselves. The latter is a natural phenomenon of EHF/THF band that may inherently improve performance of communications.

B. The Effect of Blocking

The last two figures in Fig. 6 compare the mean interference for scenarios with omnidirectional and directional antennas, when blocking is taken into account. The cone directional antenna model is used. Comparing Fig. 6(c) to Fig. 6(a), we see that the system with directional Tx or Rx antennas with blocking performs better than in case of no blocking. Similarly, the interference for system with directional Tx and Rx is lower than in case of no blocking for considered values of α.

The effect of interferers intensity on the mean interference, shown in Fig. 6(d), illustrates that the large values of λ lead to higher interference when directional antennas at Tx or Rx only are used. The reason is that the system without omnidirectional antennas is characterized by the linearly growing interference in presence of blocking, while the system with directional ones – by logarithmically growing one. For a system having directional Tx and Rx the interference is slightly lower compared to "no blocking" case, given in Fig. 6(b).

C. The Effect of Absorption

Having identified significantly higher interference in a system with directional Tx and Rx, from now on we concentrate on this system. Let us first illustrate the effect of absorption coefficient. Fig. 7 highlights dependence of the mean interference on the absorption coefficient K for cone directional antenna model with blocking. Fixing the density of interferers, λ, we observe that the interference is smaller for higher values of K, as expected, see Fig. 7(a) and Fig. 7(b). In general, when K increases, the interference naturally decreases due to less radiation reaching the receiver. It is important to note that this feature of EHF/THF band is often claimed to have negative impact rather than positive. Here, we see that proper choice of the emitted power and the operational frequency may, in fact, allow for point-to-point links creating only little interference to concurrent transmissions. Finally, Fig. 7(a) and Fig. 7(c) highlight that the effect of absorption, as expected, is similar for different directivity angles.

D. The Effect of the Antenna Model

Next we study the effect of different antenna model. Recall that according to the cone model no radiation is lost to the side lobes. The CPS model takes into account losses to side lobes via coefficient k. The question is whether the gap between these models is large to warrant additional complexity.

The mean interference as a function of the antenna directivity α for difference values of loss coefficient k is shown in Fig.

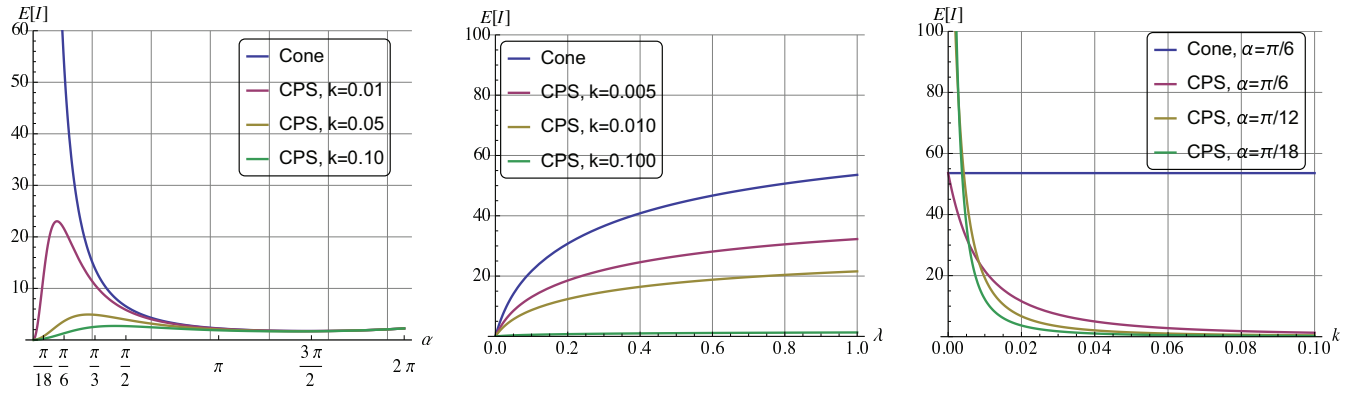

(a) Varying α, $\lambda = 1$ (b) Varying λ, $\alpha = \pi/18$ (c) Varying k, $\lambda = 1$

Fig. 8. The comparison of mean interference between cone and cone-plus-sphere antenna models.

8(a). Notice that in case of $\alpha = 0$, the CPS model rolls back to the omnidirectional one due to (9). As one may observe, the behavior of CPS model is more complicated compared to the cone one. When losses to side lobes are rather low, it expectedly resembles on the properties of the cone model. However, when k increases, the mean interference no longer tends to the function characterizing the omnidirectional case. The dependence on λ is illustrated in Fig. 8(b). As one may observe, when losses to side lobes increases the interference decreases, i.e., the cone model greatly overestimates the actual interference for a wide range of λ. Fig. 8(c) illustrates this effect for a wide range of k and different α. Since realistic antennas are non-perfect, characterized by k in the range $0.1 \sim 0.2$ [16], the simple cone model does not provide a very accurate approximation.

V. Conclusions

In this paper, we characterized the effects of the type of antenna model and antenna directivity, molecular absorption and blocking on the mean interference in wireless communication systems operating in EHF/THF bands in an "uncontrolled" random Poisson deployment. We observed that for the same emitted power, the interference in a system with directional antennas drastically increases when directivity angle increases. The blocking significantly reduces the magnitude of interference for all considered cases. Finally, the impact of molecular absorption has been shown, highlighting that proper selection of the operational frequency can help to further reduce the interference at the receiver.

We note that interference alone does not allow to make ultimate conclusion about the performance of EHF/THF systems, as the received power of the useful signal increases with the antennas directivity angle as well. In our future work, we will address signal-to-interference-plus-noise ratio as a more representative characteristic as well as capacity metrics associated with such systems.

Acknowledgement

This work was supported by Academy of Finland FiDiPro program "Nanocommunication Networks", 2012 – 2016. Dr. J. M. Jornet acknowledges the support of AFRL, under AFRL Grant No. FA8750-15-1-0050. V. Petrov acknowledges the support by Nokia Foundation.

References

[1] Cisco, "Cisco visual networking index: Global mobile data traffic forecast update, 2014-2019," 2015.
[2] Qualcomm, "The 1000x mobile data challenge," tech. rep., 2013.
[3] S. Rey, "TERAPAN: Ultra-high data rate transmission with steerable antennas at 300 GHz," IEEE 802.15-15-0167-02-0thz, Mar. 2015.
[4] J. Boyd, "Fujitsu makes a THz receiver small enough for a smartphone." http://www.spectrum.ieee.org/tech-talk/telecom/wireless/fujitsu-makes-a-terahertz-receiver-small-enough-for-a-smartphone, Oct. 2015.
[5] V. Petrov, D. Moltchanov, and Y. Koucheryavy, "Applicability assessment of terahertz information showers for next-generation wireless networks," in *IEEE International Conference on Communications (ICC)*, pp. 1–7, May 2016.
[6] I. F. Akyildiz, J. M. Jornet, and C. Han, "Terahertz band: Next frontier for wireless communications," *Physical Communication*, vol. 12, pp. 16–32, 2014.
[7] M. Akdeniz, Y. Liu, M. Samimi, S. Sun, S. Rangan, T. Rappaport, and E. Erkip, "Millimeter wave channel modelingand cellular capacity evaluation," *IEEE Journal on Selected Areas in Communications*, vol. 32, pp. 1164–1179, June 2014.
[8] M. Gapeyenko, A. Samuylov, M. Gerasimenko, D. Moltchanov, S. Singh, E. Aryafar, S. Yeh, N. Himayat, S. Andreev, and Y. Koucheryavy, "Analysis of human body blockage in millimeter-wave wireless communications systems," in *IEEE International Conference on Communications (ICC)*, May 2016.
[9] V. Petrov, D. Moltchanov, and Y. Koucheryavy, "On the efficiency of spatial channel reuse in ultra-dense thz networks," in *IEEE Global Communications Conference (GLOBECOM)*, pp. 1–7, Dec 2015.
[10] J. M. Jornet and I. F. Akyildiz, "Channel modeling and capacity analysis for electromagnetic wireless nanonetworks in the terahertz band," *IEEE Trans. Wir. Comm.*, vol. 10, pp. 3211–3221, Oct. 2011.
[11] J. M. Jornet and I. F. Akyldiz, "Femtosecond-long pulse-based modulation for terahertz band communication in nanonetworks," *IEEE Trans. Comm.*, vol. 62, pp. 1742–1754, May 2014.
[12] www.cfa.harvard.edu, "Hitran: High-resolution transmission molecular absorption database," tech. rep., Harvard-Smithson Center for Astrophysics, 2014.
[13] S. Ross, *Introduction to probability models*. Academic Press, 2010.
[14] D. R. Cox, *Renewal theory*. Methuen and Co ltd., 1970.
[15] J. Andrews, S. Buzzi, W. Choi, S. Hanly, A. Lozano, A. Soong, and J. Zhang, "What will 5G be?," *IEEE Journal on Selected Areas in Communications*, vol. 32, no. 6, pp. 1065–1082, 2014.
[16] T. Rappaport, *Wireless Communications: Principles and Practice*. Prentice Hall, 2002.